Clinical Investigations

Respiration

Respiration 2016;92:90–97
DOI: 10.1159/000448120

Received: March 25, 2016
Accepted after revision: June 27, 2016
Published online: August 23, 2016

Oxygen Desaturation Index Estimation through Unconstrained Cardiac Sympathetic Activity Assessment Using Three Ballistocardiographic Systems

Da Woon Jung[a] Su Hwan Hwang[a] Yu Jin Lee[b] Do-Un Jeong[b]
Kwang Suk Park[c]

[a]Interdisciplinary Program for Biomedical Engineering, Seoul National University Graduate School, [b]Department of Psychiatry and Behavioral Science, Seoul National University College of Medicine and Center for Sleep and Chronobiology, Seoul National University Hospital, and [c]Department of Biomedical Engineering, Seoul National University College of Medicine, Seoul, South Korea

Key Words
Nocturnal hypoxemia · Oxygen desaturation index · Cardiac sympathetic activity · Heart rate variability · Ballistocardiography

Abstract
Background: Nocturnal hypoxemia, characterized by abnormally low oxygen saturation levels in arterial blood during sleep, is a significant feature of various pathological conditions. The oxygen desaturation index, commonly used to evaluate the nocturnal hypoxemia severity, is acquired using nocturnal pulse oximetry that requires the overnight wear of a pulse oximeter probe. ***Objectives:*** This study aimed to suggest a method for the unconstrained estimation of the oxygen desaturation index. ***Methods:*** We hypothesized that the severity of nocturnal hypoxemia would be positively associated with cardiac sympathetic activation during sleep. Unconstrained heart rate variability monitoring was conducted using three different ballistocardiographic systems to assess cardiac sympathetic activity. Overnight polysomnographic and ballistocardiographic recording pairs were collected from the 20 non-nocturnal hypoxemia (oxygen desaturation index <5 events/h) subjects and the 76 nocturnal hypoxemia patients. Among the 96 recording pairs, 48 were used as training data and the remaining 48 as test data. ***Results:*** The regression analysis, performed using the low-frequency component of heart rate variability, exhibited a root mean square error of 3.33 events/h between the estimates and the reference values of the oxygen desaturation index. The nocturnal hypoxemia diagnostic performance produced by our method was presented with an average accuracy of 96.5% at oxygen desaturation index cutoffs of ≥5, 15, and 30 events/h. ***Conclusions:*** Our method has the potential to serve as a complementary measure against the accidental slip-out of a pulse oximeter probe during nocturnal pulse oximetry. The independent application of our method could facilitate home-based long-term oxygen desaturation index monitoring.

KARGER

© 2016 S. Karger AG, Basel
0025–7931/16/0922–0090$39.50/0

E-Mail karger@karger.com
www.karger.com/res

Kwang Suk Park
713, Fundamental Medical Research Building
Seoul National University College of Medicine
103 Daehak-ro, Jongno-gu, Seoul (South Korea)
E-Mail pks@bmsil.snu.ac.kr

Introduction

Nocturnal hypoxemia is characterized by abnormal reductions in the percent saturation of oxyhemoglobin in arterial blood during sleep. The oxygen desaturation index (ODI) is commonly used to evaluate the severity of nocturnal hypoxemia. The ODI is defined as the number of episodes of oxygen desaturation per hour of sleep, with oxygen desaturation defined as a decrease in blood oxygen saturation (Sp_{O_2}) to lower than 3% below baseline. Baseline is determined by computing the average Sp_{O_2} during the first 3 min of recording [1].

The significance of the ODI as quantitative feature of various pathological conditions has been documented in previous studies. Hayashi et al. [2] reported that the ODI showed a significant positive correlation with the severity of coronary atherosclerosis in patients with cardiovascular disease. Muraki et al. [3] classified middle-aged Japanese participants into three groups according to their ODI. Compared to a non-nocturnal hypoxemia (ODI <5) group, the development of type 2 diabetes was 1.5-fold higher in the mild nocturnal hypoxemia (5 ≤ ODI <15) group and 2.5-fold higher in the moderate-to-severe nocturnal hypoxemia (ODI ≥15) group. Yaffe et al. [4] showed a significant association between ODI (>15) due to sleep-disordered breathing and the risk of mild cognitive impairment or dementia. Little et al. [5] reported an elevated ODI (>15) in one third of sickle cell disease patients.

Nocturnal pulse oximetry is the gold standard for acquiring ODI. However, wearing a pulse oximeter probe overnight can cause discomfort and inconvenience. This study aimed to devise a method for the unconstrained estimation of ODI. To achieve our aim, we focused on identifying a physiological parameter that can reliably reflect the effect of nocturnal hypoxemia and can be acquired unobtrusively.

Nocturnal hypoxemia is associated with arousal events that occur to restore a normal level of oxygen saturation [6]. The occurrence of arousal events causes a marked increase in cardiac sympathetic activity [7]. We hypothesized that more severe nocturnal hypoxemia would be associated with stronger nocturnal cardiac sympathetic activation.

Heart rate variability (HRV) monitoring through ballistocardiography was considered as a method for the unconstrained assessment of cardiac sympathetic activity. HRV is a widely used noninvasive indicator reflecting the activity of the sympathetic and vagal components of the autonomic nervous system on the sinus node of the heart [8]. Ballistocardiography is a technique used to record the mechanical recoil of the body in reaction to the ejection of blood from the heart and through the vasculature [9]. Unlike electrocardiography, ballistocardiography is achievable without the attachment of electrodes to the skin, thus allowing unconstrained cardiac activity monitoring.

Materials and Methods

Participants

This study was approved by the Institutional Review Board of the Seoul National University Hospital (IRB No. 1205-048-409). All participants provided written informed consent. Two groups of participants were recruited through the Center for Sleep and Chronobiology of the Seoul National University Hospital between July 2012 and August 2015. The first group consisted of the participants without suspected nocturnal hypoxemia. The second group included the participants with suspected nocturnal hypoxemia. The inclusion criteria for both groups were (1) 20 years ≤ age <60 years and (2) 18.5 ≤ body mass index <40. The exclusion criteria for both groups were (1) the presence of contact allergic reactions to Ag/AgCl electrode, (2) the presence of lesions such as infection and surgical wound on the skin in contact with electrode, (3) the presence of unstable vital signs, (4) the presence of parasomnia, sleep-related movement disorders, or circadian rhythm sleep disorders, (5) the presence of major behavioral or neurological disorders, and (6) the use of medications known to influence sleep or autonomic nervous system function. Twenty and 77 participants who met the inclusion and exclusion criteria were included in the first and the second groups, respectively. All participants in the second group were the subjects who had been referred for polysomnography (PSG) because of suspected sleep-related breathing disorders.

Polysomnography

Standard nocturnal PSG was performed at the Center for Sleep and Chronobiology of the Seoul National University Hospital. The physiological recordings acquired during PSG were electroencephalogram at the positions F4-M1, C4-M1, and O2-M1, bilateral electrooculogram, electromyogram at the chin and anterior tibialis muscles, electrocardiogram (ECG) at lead II, body posture using a tri-axis accelerometer, nasal pressure using a nasal cannula/pressure transducer, oronasal airflow using a thermistor, thoracic and abdominal volume changes using piezoelectric-type belts, snoring sounds using a microphone, and Sp_{O_2} using a pulse oximeter (Respironics Novametrix MARSSp_{O_2}, Wallingford, Conn., USA). The pulse oximeter was worn on the index finger of the nondominant hand. All of the data, except for Sp_{O_2}, were sampled at 250 Hz. The sampling rate for Sp_{O_2} data was 1 Hz.

Sleep parameters were evaluated by certified sleep technologists and verified by sleep physicians in accordance with the 2007 American Academy of Sleep Medicine (AASM) manual [10]. After artifacts had been removed from overnight Sp_{O_2} data by eliminating all changes >4%/s and removing any Sp_{O_2} <50%, the ODI reference values were determined [11].

Unconstrained Ballistocardiography

Overnight ballistocardiography using a piezoelectric sensor was conducted simultaneously with PSG for the unconstrained acquisition of heartbeat data. Three types of piezoelectric sensors, i.e. a load-cell, a polyvinylidene fluoride (PVDF) film sensor, and an electromechanical film (EMFi) sensor, were used in the different ballistocardiogram (BCG) acquisition systems. Using each type of piezoelectric sensor, 20 (20.6%), 61 (62.9%), and 16 (16.5%) recordings, respectively, were acquired with a sampling rate of 250 Hz. The load-cell-installed bed system for acquiring BCG was equipped with four-strain gauge-based load cells underneath each bed leg [12, 13]. The PVDF film [14] and the EMFi sensor-based BCG acquisition systems, respectively, consisted of a 300 (length) × 300 (width) × 0.1 (height) mm PVDF film sensor and a 580 × 400 × 0.4 mm EMFi sensor. In each film sensor-based BCG acquisition system, the PVDF film or the EMFi sensor was placed between the mattress and the bed cover under the dorsal surface. Because both the PVDF film and the EMFi sensors were sufficiently thin and flexible, the ability of the sensors to interfere with sleep was very low.

Cardiac Sympathetic Activity Assessment

Because nocturnal hypoxemia is not a phenomenon observed during wakefulness, the method developed in our previous study for detecting nocturnal awakenings was applied to the piezoelectric signals [14]. After obtaining BCG from the piezoelectric signals using a fifth-order IIR Butterworth band-pass filter (0.5–35 Hz), the J-peaks on BCG were detected. By counting the number of J-peaks in each epoch (30-second segment), awakening epochs were identified based on the hypothesis that unexpected absence of J-peaks would be caused by empty bed or body movement producing BCG waveform distortion, which is related to the wakefulness state. For the epochs with a sufficient number of J-peaks, identification of awakening epochs was performed based on the effect of sleep involving significantly slower heart rate (HR) compared with the HR observed during wakefulness. After excluding the BCG acquired during the determined awakening epochs, the later analyses were carried out.

To assess cardiac sympathetic activity, BCG-based HRV was analyzed using nonlinear and time- and frequency-domain analyses. Prior to extracting HRV parameters, time series of normal-to-normal sinus (N-N) intervals were obtained by processing outliers in the BCG inter-beat intervals. Outliers caused by false or missed beat detections were identified by a moving window of 41-data point length. Central points lying outside 20% of the window average were eliminated [15].

Three HRV nonlinear parameters, i.e. SD1, SD2 (standard deviations of the Poincaré plot), and SampEn (sample entropy), were investigated. The extracted HRV time-domain parameters were as follows: SDNN (standard deviation of N-N intervals), RMSSD (square root of the mean squared differences between successive N-N intervals), NN50 (number of successive N-N interval pairs that differ by more than 50 ms), and pNN50 (NN50 divided by the total number of N-N intervals). The HRV frequency-domain analysis was conducted according to the following procedure. The N-N interval time series were resampled at 4 Hz using a cubic spline interpolation. Within the 1,024-sample window, data in each of the 3 overlapping 512-sample subwindows were linearly detrended and windowed using a Hamming function. Spectral power was computed over the 1,024-sample window using a fast Fourier transform. The 1,024-sample window was advanced by 512 samples, and the calculation was repeated until the entire N-N interval time series was analyzed [15]. Finally, the following three HRV parameters, LF_{tm}, HF_{tm}, and LF_{tm}/HF_{tm}, were computed from each BCG recording.

$$LF_{tm} = \frac{1}{N}\sum_{i=1}^{N}\left(P_{LF1_i} + P_{LF2_i}\right)$$

$$HF_{tm} = \frac{1}{N}\sum_{i=1}^{N}\left(P_{HF1_i} + P_{HF2_i}\right)$$

$$LF_{tm} / HF_{tm} = \frac{1}{N}\sum_{i=1}^{N}\left(\frac{P_{LF1_i} + P_{LF2_i}}{P_{HF1_i} + P_{HF2_i}}\right),$$

where P_{LF1i} and P_{LF2i} are the spectral power values at the first and second maximal peaks in the low-frequency (LF) band (0.04–0.15 Hz) for the i^{th} window, respectively. P_{HF1i} and P_{HF2i} are the first and second maximal peaks power in the high-frequency (HF) band (0.15–0.4 Hz) for the i^{th} window, respectively. N is the total number of the windows in the BCG recording. A very-low-frequency band (0.003–0.04 Hz) component was not extracted to avoid dubious interpretation, caused by the insufficient length of the data to be analyzed [16].

Results

Participants

From the PSG results, all participants without suspected nocturnal hypoxemia were confirmed as non-nocturnal hypoxemia (ODI <5) subjects. All participants with suspected nocturnal hypoxemia were determined as nocturnal hypoxemia (ODI ≥5) patients. Among a total of 97 participants who performed overnight ballistocardiography along with PSG, 1 participant exhibiting an abnormally poor sleep efficiency of 65% was excluded from the analysis. As a result, study subjects consisted of 20, 22, 24, and 30 individuals with non-nocturnal hypoxemia, mild nocturnal hypoxemia (5 ≤ ODI <15), moderate nocturnal hypoxemia (15 ≤ ODI <30), and severe nocturnal hypoxemia (ODI ≥30), respectively. The demographic and anthropometric characteristics and sleep parameters for the four groups are summarized in table 1. No significant differences were observed in any of the demographic and anthropometric parameters among the four groups (Kruskal-Wallis test, all $p > 0.05$). The difference in ODI was significant among the four groups (Kruskal-Wallis test, $p < 0.05$).

Table 1. Summary of subject characteristics and polysomnography results

	Non-nocturnal hypoxemia	Mild nocturnal hypoxemia	Moderate nocturnal hypoxemia	Severe nocturnal hypoxemia
Sample size (male/female)	20 (15/5)	22 (18/4)	24 (18/6)	30 (22/8)
Age, years	45.7±10.6	47.3±8.8	46.9±9.3	47.0±10.2
BMI	24.4±2.6	24.2±2.1	25.7±3.7	25.9±3.6
ODI, events/h	1.7±1.4	10.1±3.0	22.2±4.5	49.5±14.5
TRT, min	492.2±35.6	494.1±33.8	495.3±27.6	494.5±29.0
TST, min	462.2±41.1	457.6±34.7	452.2±27.4	445.6±28.2
SL, min	5.6±5.4	6.0±4.6	5.1±3.7	4.8±4.0
WASO, min	24.2±15.0	29.8±15.4	37.8±11.6	44.0±12.2
SE, %	93.6±3.4	92.6±3.2	91.0±2.7	89.8±2.8

BMI = Body mass index; TRT = total recording time; TST = total sleep time; SL = sleep latency; WASO = wake after sleep onset; SE = sleep efficiency. Subjects were classified according to their ODI values into non-nocturnal hypoxemia (ODI <5), mild nocturnal hypoxemia (5 ≤ ODI <15), moderate nocturnal hypoxemia (15 ≤ ODI <30), and severe nocturnal hypoxemia (ODI ≥30) groups. Data are presented as the means ± SD.

BCG Reliability

Figure 1 shows simultaneously recorded ECG and BCG tracings with the respective N-N interval time series obtained from ECG and BCG. When the BCG-derived N-N interval time series were classified according to the BCG acquisition system, Pearson's *r* values (mean ± SD) of 0.96 ± 0.01, 0.95 ± 0.01, and 0.95 ± 0.01 were reported between the ECG-derived N-N interval time series and the BCG-derived N-N interval time series obtained from the load-cell-installed bed and the PVDF film and the EMFi sensor-based systems, respectively. The differences in Pearson's *r* were not significant (Kruskal-Wallis test, all $p > 0.05$).

ODI Estimation

The correlation coefficients between the ODI and the HRV parameters are enumerated in table 2. The LF_{tm} exhibited the highest correlation coefficient with the ODI (Spearman's $\rho = 0.98$, $p < 0.01$).

All of the ODI and the LF_{tm} datasets were sorted in ascending order of the ODI. The datasets in even-numbered order were classified as the training data. As a result, among the 96 datasets, 48 datasets were included in the training set to establish a regression model and the remaining 48 datasets were included in the test set to provide an independent performance validation.

Figure 2 shows the relationship between the ODI and the LF_{tm} for the data in the training set (fig. 2, filled triangles) and in the test set (fig. 2, hollow circles). The regression analysis was performed using CurveExpert Professional software (v.2.0.4, www.curveexpert.net, USA) with a significant probability level of 95%. In the regres-

Table 2. Correlation coefficients between ODI and HRV parameters

HRV parameter	Spearman's ρ	p value
SD1 (ms)	0.54	<0.01
SD2 (ms)	0.50	<0.01
SampEn	0.13	n.s.
SDNN (ms)	0.65	<0.01
RMSSD (ms)	0.66	<0.01
NN50 (count)	0.60	<0.01
pNN50 (%)	0.62	<0.01
LF_{tm} (ms^2)	0.98	<0.01
HF_{tm} (ms^2)	–0.41	<0.01
LF_{tm}/HF_{tm}	0.80	<0.01

n.s. = No significance; SD1 and SD2 = standard deviations of the Poincaré plot; SampEn = sample entropy; SDNN = standard deviation of N-N intervals; RMSSD = square root of the mean squared differences between successive N-N intervals; NN50 = number of successive N-N interval pairs that differ more than 50 ms; pNN50 = NN50 divided by the total number of N-N intervals; LF_{tm} = average of the sums of the 2 maximal power peaks in the HRV LF band (0.04–0.15 Hz); HF_{tm} = average of the sums of the 2 maximal power peaks in the HRV HF band (0.15–0.4 Hz).

Table 3. Parameters of the regression model used to estimate ODI

Explanatory variable (*x*)	Fitting function	Fitting parameter		
		a	b	c
LF_{tm} (ms^2)	$\frac{a \times x^b}{c^b + x^b}$	121.28	1.86	891.97

LF_{tm} = Average of the sums of the 2 maximal power peaks in the HRV LF band (0.04–0.15 Hz).

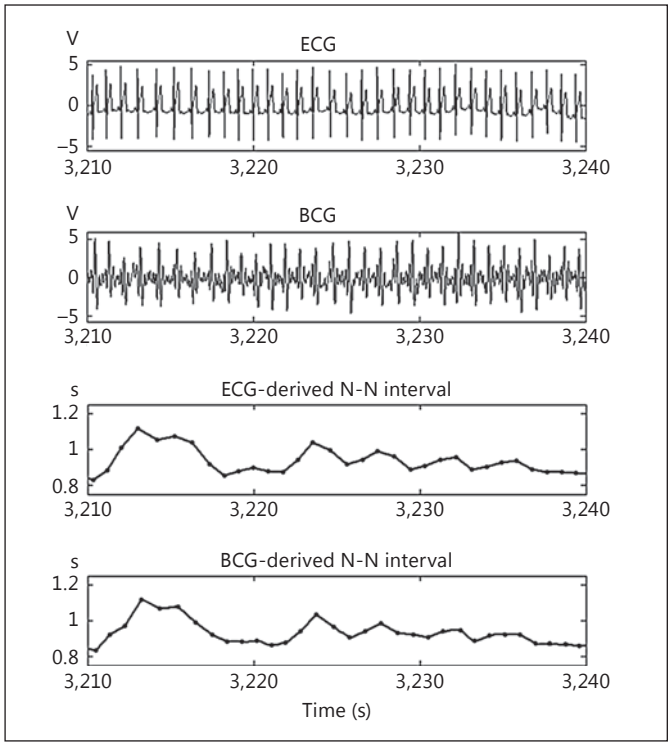

Fig. 1. Simultaneously recorded ECG and BCG with N-N intervals acquired from ECG and BCG data, respectively.

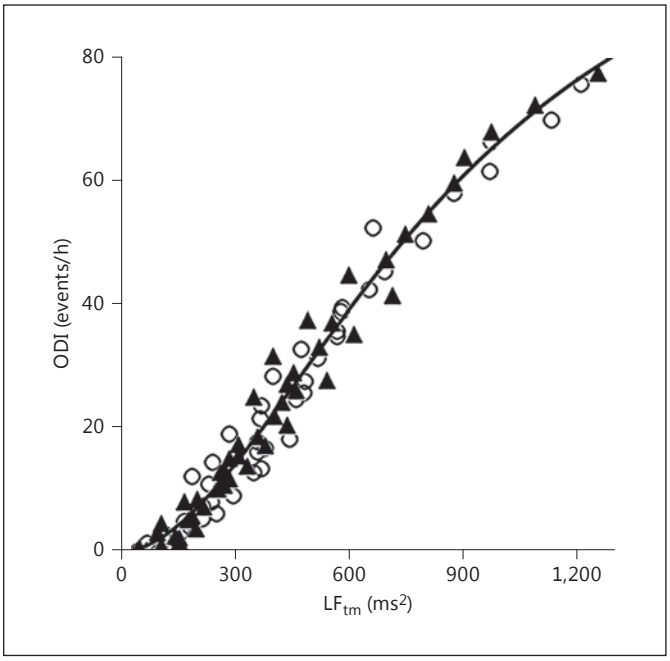

Fig. 2. Scatter plot showing the relationship between the average of the sums of the 2 maximal power peaks in the HRV LF band (LF_{tm}) and the ODI (training data, filled triangles; test data, hollow circles). The best-fitting curve (solid line) of the training data was derived from the Hill model.

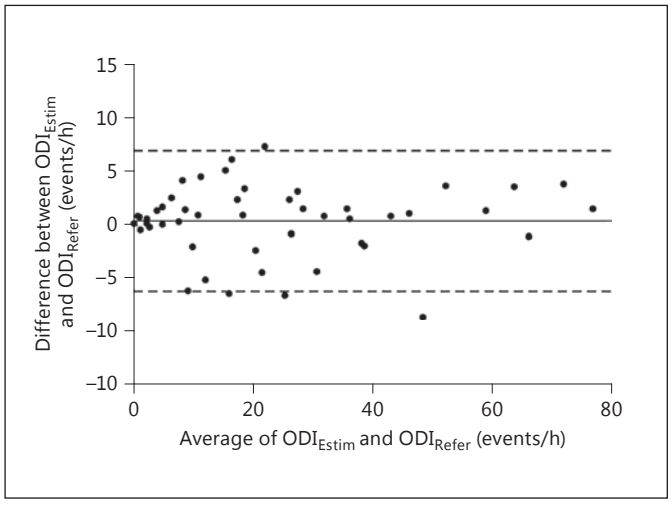

Fig. 3. Bland-Altman plot of the differences between the ODI estimates obtained by our method (ODI_{Estim}) and the ODI reference values determined by nocturnal pulse oximetry (ODI_{Refer}) against the averages for the test data. The solid line represents the mean of differences between the ODI_{Estim} and ODI_{Refer} and the dashed lines denote the 95% limits of agreement (±2 × SD of the differences).

sion modeling, the dependent and explanatory variables were the ODI and LF_{tm}, respectively. The best-fitting curve (fig. 2, solid line) to the training data was derived from the Hill model with a determination coefficient (R^2) of 0.98. The representation of the best-fitting model is summarized in table 3.

ODI Estimation and Nocturnal Hypoxemia Diagnostic Performance Evaluation

Between the estimates and the reference values of the ODI, root mean square errors of 3.14 and 3.33 events/h were acquired for the training and the test sets, respectively. Pearson's *r* values between the ODI estimates and the reference values were 0.99 ($p < 0.01$) for both training and test sets.

Figure 3 shows the Bland-Altman plot of the differences between the estimates and the reference values of the ODI against the averages for the test set. The mean of the differences between the estimates and the reference values of the ODI was computed at 0.46 events/h (fig. 3, solid line). Between the ODI estimates and the reference values, the 95% limits of agreement were observed from –6.06 to 6.98 events/h (fig. 3, dashed lines).

Table 4. Nocturnal hypoxemia diagnostic performance at different ODI cutoffs (events/h)

	ODI cutoff value		
	≥5	≥15	≥30
Sensitivity, %	100.0	96.3	93.3
Specificity, %	90.0	90.5	100.0
PPV, %	97.4	92.9	100.0
NPV, %	100.0	95.0	97.1
Accuracy, %	97.9	93.8	97.9
Cohen's kappa coefficient	0.93	0.87	0.95
ROC-AUC	1.00	0.99	1.00

PPV = Positive predictive value; NPV = negative predictive value; ROC-AUC = area under the receiver operating characteristics curve. Cohen's kappa coefficients ranging from 0.81 to 1.00 indicate almost perfect agreement.

Table 4 includes the nocturnal hypoxemia diagnostic performance produced by our method at ODI cutoffs of ≥5, 15, and 30 events/h. For the test set, the averages for the three different ODI cutoffs were sensitivity 96.5%, specificity 93.5%, positive predictive value 96.8%, negative predictive value 97.4%, accuracy 96.5%, Cohen's kappa coefficient 0.92 corresponding to almost perfect agreement, and area under the receiver operating characteristics curve 1.00.

Discussion

To our knowledge, this is the first study that suggests a novel method for providing ODI without using nocturnal pulse oximetry. Not requiring the overnight wear of a pulse oximeter probe to obtain ODI is useful for long-term monitoring of nocturnal hypoxemia.

Our approach to the wholly unconstrained estimation of ODI was implemented using BCG-based HRV analysis. For the N-N intervals acquired during sleep, HRV analysis was employed to assess cardiac sympathetic activity, assumed to reflect nocturnal hypoxemia severity. Piezoelectric sensor-based BCG monitoring systems were used for the unconstrained acquisition of N-N intervals. With a growing need for long-term monitoring techniques in sleep studies, ballistocardiography has been suggested as a measure for providing information on cardiac activity without disturbing sleep in an out-of-sleep laboratory environment [13, 14, 17–24]. Many previous studies validated the usefulness of ballistocardiography for overnight heartbeat monitoring [14, 17–20, 22, 23]; however, no study has attempted to use ballistocardiographic recording for the unconstrained estimation of the ODI.

To represent the difference in the HRV power spectral components according to the ODI, sleep spectrograms were generated by fast Fourier transform computation of the BCG-derived N-N interval time series. Figure 4 illustrates the top and side view of 3D sleep spectrograms obtained from two individuals belonging to different nocturnal hypoxemia severity groups. Compared with the sleep spectrogram of the non-nocturnal hypoxemia subject (ODI = 0.6 events/h; fig. 4a, b), the severe nocturnal hypoxemia patient (ODI = 33.0 events/h; fig. 4c, d) showed markedly increased LF components. LF components of HRV are known to reflect cardiac sympathetic activation [25]. The increased cardiac sympathetic activity in the severe nocturnal hypoxemia patient might be caused by the effective and frequent occurrence of oxygen desaturation accompanying arousal events as a regulation mechanism [26–29].

In this study, the average of the sums of the 2 maximal power peaks in the HRV LF band, denoted by LF_{tm}, was used as a predictor of ODI. Across a wide range of ODI values, from 0 to 77.3 events/h, the LF_{tm} exhibited a strong correlation with the ODI. It is notable that the ODI predictive ability of the LF_{tm} was greater than that of the conventionally used HRV parameter such as the power in the LF band and its normalized value. We surmise that our methods employed in the signal processing and the spectral analysis of the N-N interval time series were optimized for underlining predominant peaks in the periodogram, which might minimize the interference of artifacts. Furthermore, the choice of the 2 predominant power peaks in the LF band might be effective in sensitive and reliable reflection and quantification of the increase in cardiac sympathetic activity.

As shown in figure 2, a sigmoid relationship was present between the ODI and the LF_{tm}. A specific lower asymptote was observed in the sigmoid curve describing the relationship between the ODI and the LF_{tm}. The ODI and the LF_{tm} datasets near the lower asymptote represent a high variance in the LF_{tm} in the non-nocturnal hypoxemia group. As a result, nonlinear least-squares curve fitting for the relationship between the ODI and the LF_{tm} enabled a reliable estimation of the ODI not only for the mild-to-severe nocturnal hypoxemia group but also for the non-nocturnal hypoxemia group.

For the subjects whose nocturnal hypoxemia severity was overestimated, the differences between each ODI es-

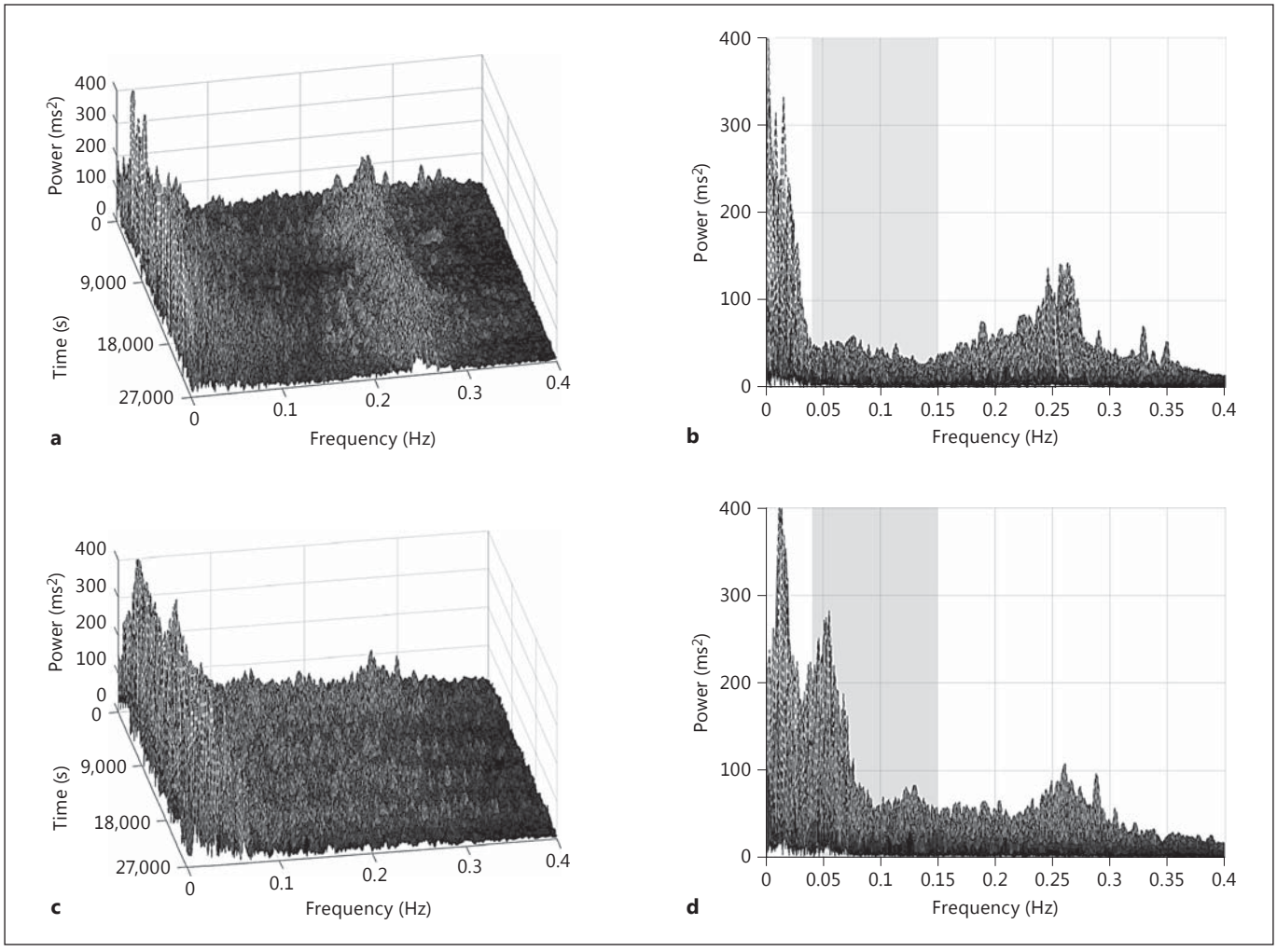

Fig. 4. 3D sleep spectrograms of a non-nocturnal hypoxemia subject [overhead view (**a**); lateral view (**b**)] and a patient with severe nocturnal hypoxemia [overhead view (**c**); lateral view (**d**)]. The gray blocks in **b** and **d** indicate the HRV LF band (0.04–0.15 Hz).

timate and the upper limit of each actual nocturnal hypoxemia severity criterion on ODI were explored, and they showed an average value of 2.62 events/h. In the subjects whose nocturnal hypoxemia severity was underestimated, the average difference between each ODI estimate and the lower limit of each actual nocturnal hypoxemia severity criterion on ODI was 1.94 events/h. This suggests a high possibility of the subjects whose nocturnal hypoxemia severity was misclassified by our method to be found in the 'gray zone' where the ODI values around a discrete boundary between contiguous severity groups are included.

Our method has the potential to serve as a complementary measure against the accidental detachment of a pulse oximeter probe from the body because of toss and turn during nocturnal pulse oximetry. A home-based long-term follow-up study of nocturnal hypoxemia patients may be facilitated by measuring night-to-night ODI variability using our method.

One limitation of our study is the relatively small sample size. Analyzing a greater number of pulse oximetric and ballistocardiographic recording pairs is necessary to improve the generalizability of our method. Another limitation is associated with the reproducibility. Because all data analyzed in this study were obtained from in-laboratory recordings, applying our method to at-home multi-night recordings is required. The applicability of ballistocardiographic recording to the estima-

tion of other indices derived from nocturnal pulse oximetry, such as cumulative time with low oxygen saturation (e.g., CT90, CT80) and delta index, will be studied in future work.

Acknowledgements

This work was supported by a National Research Foundation of Korea (NRF) grant funded by the Ministry of Science, ICT & Future Planning (No. NRF-2012R1A2A2A02010714).

References

1 Gyulay S, Olson LG, Hensley MJ, King MT, Allen KM, Saunders NA: A comparison of clinical assessment and home oximetry in the diagnosis of obstructive sleep apnea. Am Rev Respir Dis 1993;147:50–53.

2 Hayashi M, Fujimoto K, Urushibata K, Uchikawa S-I, Imamura H, Kubo K: Nocturnal oxygen desaturation correlates with the severity of coronary atherosclerosis in coronary artery disease. Chest 2003;124:936–941.

3 Muraki I, Tanigawa T, YamagishiK K, Sakurai S, Ohira T, Imano H, Kitamura A, Kiyama M, Sato S, Shimamoto T: Nocturnal intermittent hypoxia and the development of type 2 diabetes: the Circulatory Risk in Communities Study (CIRCS). Diabetologia 2010;53:481–488.

4 Yaffe K, Laffan AM, Harrison SL, Redline S, Spira AP, Ensrud KE, Ancoli-Israel S, Stone KL: Sleep-disordered breathing, hypoxia, and risk of mild cognitive impairment and dementia in older women. JAMA 2011;306:613–619.

5 Little JA, Rotz S, Kim C, O'Riordan M, Langer N, Lance C: Nocturnal hypoxemia (not sleep apnea) may drive reticulocytosis in sickle cell disease. Blood 2014;124:1384–1384.

6 Levitzky MG: Using the pathophysiology of obstructive sleep apnea to teach cardiopulmonary integration. Adv Physiol Educ 2008;32:196–202.

7 Zoccali C, Mallamaci F, Tripepi G: Traditional and emerging cardiovascular risk factors in end-stage renal disease. Kidney Int 2003;63:S105–S110.

8 Sztajzel J: Heart rate variability: a noninvasive electrocardiographic method to measure the autonomic nervous system. Swiss Med Wkly 2004;134:514–522.

9 Weissler AM: Ballistocardiography; in Weissler AM (ed): Noninvasive Cardiology. New York, Grune and Stratton, 1973, pp 301–368.

10 Iber C, Ancoli-Israel S, Chesson A, Quan SF: The AASM Manual for the Scoring of Sleep and Associated Events: Rules, Terminology and Technical Specifications, ed 1. Westchester, American Academy of Sleep Medicine, 2007.

11 Magalang UJ, Dmochowski J, Veeramachaneni S, Draw A, Mador MJ, El-Solh A, Grant BJ: Prediction of the apnea-hypopnea index from overnight pulse oximetry. Chest 2003;124:1694–1701.

12 Choi BH, Chung GS, Lee J-S, Jeong D-U, Park KS: Slow-wave sleep estimation on a load-cell-installed bed: a non-constrained method. Physiol Meas 2009;30:1163–1170.

13 Jung DW, Hwang SH, Chung GS, Lee Y-J, Jeong D-U, Park KS: Estimation of sleep onset latency based on the blood pressure regulatory reflex mechanism. IEEE J Biomed Health Inform 2013;17:539–544.

14 Jung DW, Hwang SH, Yoon HN, Lee YJ, Jeong D-U, Park KS: Nocturnal awakening and sleep efficiency estimation using unobtrusively measured ballistocardiogram. IEEE Trans Biomed Eng 2014;61:131–138.

15 Thomas RJ, Mietus JE, Peng C-K, Goldberger AL: An electrocardiogram-based technique to assess cardiopulmonary coupling during sleep. Sleep 2005;28:1151–1161.

16 Heart rate variability. Standards of measurement, physiological interpretation, and clinical use. Task Force of the European Society of Cardiology and the North American Society of Pacing and Electrophysiology. Eur Heart J 1996;17:354–381.

17 Brink M, Müller CH, Schierz C: Contact-free measurement of heart rate, respiration rate, and body movements during sleep. Behav Res Methods 2006;38:511–521.

18 Chen W, Zhu X, Nemoto T, Kanemitsu Y, Kitamura K, Yamakoshi K-I: Unconstrained detection of respiration rhythm and pulse rate with one under-pillow sensor during sleep. Med Biol Eng Comput 2005;43:306–312.

19 Chee Y, Han J, Youn J, Park K: Air mattress sensor system with balancing tube for unconstrained measurement of respiration and heart beat movements. Physiol Meas 2005;26:413–422.

20 Wang F, Tanaka M, Chonan S: Development of a PVDF piezopolymer sensor for unconstrained in-sleep cardiorespiratory monitoring. J Intell Mater Syst Struct 2003;14:185–190.

21 Chow P, Nagendra G, Abisheganaden J, Wang Y: Respiratory monitoring using an air-mattress system. Physiol Meas 2000;21:345–354.

22 Jansen BH, Larson BH, Shankar K: Monitoring of the ballistocardiogram with the static charge sensitive bed. IEEE Trans Biomed Eng 1991;38:748–751.

23 Alihanka J, Vaahtoranta K, Saarikivi I: A new method for long-term monitoring of the ballistocardiogram, heart rate, and respiration. Am J Physiol 1981;240:R384–R392.

24 Alihanka J, Vaahtoranta K: A static charge sensitive bed. A new method for recording body movements during sleep. Electroencephalogr Clin Neurophysiol 1979;46:731–734.

25 Malik M, Bigger JT, Camm AJ, Kleiger RE, Malliani A, Moss AJ, Schwartz PJ: Heart rate variability standards of measurement, physiological interpretation, and clinical use. Eur Heart J 1996;17:354–381.

26 Pitson D, Stradling J: Autonomic markers of arousal during sleep in patients undergoing investigation for obstructive sleep apnoea, their relationship to EEG arousals, respiratory events and subjective sleepiness. J Sleep Res 1998;7:53–59.

27 Greenberg HE, Sica A, Batson D, Scharf SM: Chronic intermittent hypoxia increases sympathetic responsiveness to hypoxia and hypercapnia. J Appl Physiol 1999;86:298–305.

28 Neubauer JA: Invited review: physiological and pathophysiological responses to intermittent hypoxia. J Appl Physiol 2001;90:1593–1599.

29 Guilleminault C, Poyares D, Rosa A, Huang Y-S: Heart rate variability, sympathetic and vagal balance and EEG arousals in upper airway resistance and mild obstructive sleep apnea syndromes. Sleep Med 2005;6:451–457.